Real-time holographic interferometry through fibre optics

T D Dudderar† and **J A Gilbert**‡

† AT & T Bell Laboratories, Murray Hill, New Jersey 07974, USA

‡ Associate Professor of Engineering Mechanics, University of Wisconsin-Milwaukee, Milwaukee, Wisconsin 53201, USA

Abstract. Stable, high frequency holographic interference fringes have been recorded on objects illuminated and viewed through fibre optics in real time using a system of singlemode fibre optic illuminators, a multimode fibre optic image bundle and a lensless 'instant' holocamera. This development has great potential for applications in the full-field remote measurement of surface displacements and/or deformations as they occur.

1. Introduction

The highly sensitive full-field interferometric technique utilising optical holography can now be applied to studies of interior or otherwise inaccessible objects through the use of a mixed mode system of flexible optical fibre elements. In addition, the use of singlemode optical fibres for object and reference beam illuminators greatly simplifies the required experimental set-up for conventional holographic and holo-interferometric (HI) applications. In recent years investigators have explored the use of multimode fibre optic bundles (Rosen 1975, Gilbert and Herrick 1981, Yonemura et al 1981, Gilbert et al 1982, Rowley 1983) and individual single- or multimode optical fibres (Hadbawnik 1976. Suhara et al 1977, Leite 1979, Gilbert et al 1983a, b, Hall et al 1983, Jones et al 1984) as illuminators for CW holography (either reference beam illumination, object illumination, or both). As a result of these studies it is now apparent that individual singlemode optical fibre elements are the most stable flexible illuminators for both the object and the hologram. However, it has also been demonstrated (Gilbert and Herrick 1981, Yonemura et al 1981, Gilbert et al 1982) that transmission of a reflected object wavefront (or image) from a remote or otherwise inaccessible location to the hologram site can best be accomplished through the use of a coherent optical fibre bundle. Since all such bundles are composed of multimode optical fibres they lack the stability of singlemode elements, and must generally be shielded from the deleterious effects of mechanical motion along their length. Still, mixed (single- and multi-) mode fibre optic systems can be applied to HI studies of remote objects (Gilbert et al 1983b) and even subjects located under water (Gilbert et al 1983a). Recently, two other approaches to overcoming the mechanical stability limitations of flexible multimode fibre optics have been demonstrated. In one (Dudderar and Gilbert 1983), the extremely short (20 ns) exposure duration of a pulsed ruby laser has been used to record stable remote holograms through an all multimode fibre optic system, while in the other, ultralow spatial frequency standing wave interference patterns have been transmitted through a multimode image bundle to generate stable remote holograms (Dudderar et al 1983) and holo-interferograms (Gilbert et al 1984) using CW laser illumination through singlemode fibre optics. Fibre optic technology has also been further exploited as described in a recent report (Jones et al 1984) in which the variable beamsplitter common to most holographic systems was replaced by a fibre optic directional coupler, further simplifying the optical set-up. The same study also raised the question of thermally induced phase drift in singlemode illuminators sufficient to preclude hologram exposures of much longer than a fraction of a second, and proposed a sophisticated compensation system to overcome this problem should it arise.

2. Holographic interferometry

There are at least three different approaches to doing HI, beginning with the time averaged technique (Powell and Stetson 1965, Stetson and Powell 1965) developed to reveal contours of constant amplitude on the surface of a vibrating object. In this technique a holo-interferogram is produced by exposing a hologram for a period of time during which the test object executes many cycles of steady vibration. Quantitative analysis and interpretation of the resulting fringe fields revealed that the vibratory nodes correspond to the square of the zero-order Bessel function evaluated at zero, $J_0(0)$; the dark holographic fringes to the zeros of $J_0(Z)$, and the light holographic fringes to its maxima and minima. A second technique, usually referred to as double exposure HI, generates a high contrast fringe field by interfering two object wavefronts reconstructed from the same doubly exposed hologram. In this case dark cosine fringes appear in space around the test object. These fringes are associated with changes in optical path length (resulting from changes in the test object occurring between exposures) which in turn induce changes in phase. As such, double exposure HI provides a permanent record of the changes which occurred between exposures, but no history of information describing the changes over time as they actually occurred. Real-time HI, on the other hand, provides a cosine fringe field which changes as the test object changes. Real-time fringes are generated directly by interfering the actual coherent wavefront from the object with a reconstructed holographic 'reference' wavefront. In order to generate high contrast real-time fringes, this approach requires that the object illumination and reconstructing reference beams be adjusted to yield object wavefronts of nearly equal intensity and that both beams and the hologram be located in exactly their original positions relative to the test object during reconstruction of the reference wavefront. This latter (most critical) requirement can be met, though often with some difficulty, by precise repositioning of the hologram after its removal for processing elsewhere, or, more effectively, by processing the hologram in place (*in situ* processing). In recent years the development of so-called 'instant' holographic recording systems has greatly facilitated the latter approach. Consequently, even without the flexibility and convenience of fibre optics, real-time HI has become one of the more powerful techniques for continuously monitoring the deformation of an object as it takes place, and without the need to resort to any special surface preparation (e.g. polishing to optical flatness, as with conventional interferometry, or marking, as with moire techniques). Nevertheless, to date all sophisticated HI applications involving the use of optical fibre elements in 'remote' or mixed mode systems have involved either the double exposure and/or the time averaged technique (Dudderar et al 1984), and no stable real-time systems have been reported.

In the present study we demonstrate the first use of a mixed mode fibre optic holographic interferometer with sufficient stability to monitor full-field rigid body motion and/or surface deformation on an obscured test subject in real time.

3. The real-time fibre optic holographic interferometry system

Figure 1 shows a schematic diagram of the type of mixed mode real-time fibre optic holographic interferometry (RTF–HI) system used in this study. Here the light from a 30 mW CW laser ($\lambda = 0.633\,\mu m$) is divided into two beams by a variable beam splitter and launched through low power objectives into two singlemode optical fibres, one (1650 mm long) arranged to illuminate an obscured object and the other (2480 mm long) arranged to illuminate the hologram itself†. A short (45 mm) focal length wide aperture lens is used to capture light reflected from the test subject and image it (at a tenfold reduction in size) onto one end of the fibre optic image bundle‡ which transmits the image back to the hologram area. A real-time 'instant' holocamera (situated 40 mm from the unlensed output end of the image bundle) is used to holographically record the light emerging from the end of the bundle during a 5 s exposure.
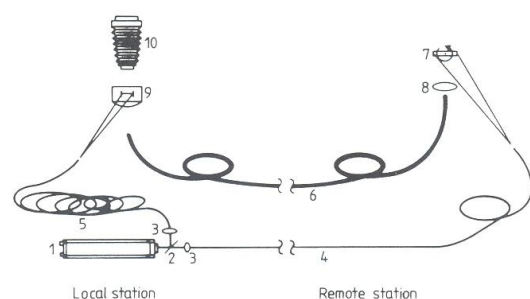

Figure 1. Schematic of the real-time fibre optic holographic interferometry system (RTF-HI system) used in these experiments. 1, continuous wave laser; 2, variable beamsplitter; 3, low power objective; 4, singlemode optical fibre object illumination beam; 5, singlemode optical fibre reference beam; 6, multimode optical fibre image transmitting bundle; 7, test subject in gimballed mount; 8, imaging lens; 9, holocamera; 10, interferogram camera.

This single exposed Fraunhofer type hologram may then be reconstructed to reproduce the original image of the subject as it was transmitted through the image bundle. Subsequent re-illumination of the test subject itself provides a remote view, observable through the output end of the image bundle, of the test subject, as it was and as it is. Since both this 'as it is' real-time view and the 'as it was' holographically reconstructed view are complete in terms of both amplitude and phase, they will interfere in real time as would any pair of directly observed and reconstructed HI wavefronts. Consequently, as the object surface is displaced, either by rigid body movement or by deformation, a pattern of real-time interference fringes appears. These fringes result from constructive and destructive interference due to phase differences associated with the displacement induced changes in the optical path lengths of the coherent wavefronts (images) as seen through the hologram.

† Losses through the singlemode fibres run around 50–60%, most of which occurs at the launch.
‡ This was a flexible coherent fibre optic bundle of $33\,\mu m$ resolution, approximately 1 m long and 10 mm in diameter, manufactured by Americal ACMI of Stanford, Connecticut. Loss through the bundle runs around 75–80%.

Moreover, as in conventional real-time HI their distribution in space may be related to the wavelength and geometry of illumination and observation, and the displacement of the surface (Collier *et al* 1971, Erf 1974, Caufield 1979, Vest 1979, Abramson 1981). In the present experiment the RTF-HI system is arranged† so that the resulting cosine fringes are the loci of constant normal or out-of-plane surface displacement with a fringe-to-fringe sensitivity of $0.3174\,\mu m$ at a wavelength of $0.633\,\mu m$.

These fringe fields appear to form in space on or near the output end of the image bundle, and were recorded on polaroid film with a camera focused in that area through a 135 mm lens operated in the range from f4 to f5.6. This camera was arranged to give a ninefold magnification from the end of the image bundle to the interferogram recording plane, for an overall magnification of approximately 0.9 through the entire system. Somewhat smaller scale reproductions of these interference fringe fields are shown in figures 2, 3 and 4 for the various rigid body rotations and deformations described below.

4. Experiment

Most of these tests were conducted on a subject which consisted of a 1.6 mm thick glass disc‡ of 88 mm diameter bonded around its circumference (leaving 80 mm free diameter) to a stiff ring mounted in a two axes gimballed holder with a central loading micrometer§. Also, most were run in real time with a few holographic double exposures added for comparison purposes. Figures 2(*a*), (*b*) and (*c*) show the interferometric fringe fields recorded in real time as the disc was tilted about a horizontal axis at angles of 0.0025°, 0.0112° and 0.0160° (respectively) from its reference position. For comparison figure 2(*d*) shows a fringe field obtained by double exposure holographic interferometry with the disc tilted 0.0027° between exposures, a result quite like the real-time result at a comparable tilt shown in figure 2(*a*). Figures 3(*a*), (*b*) and (*c*) show real-time interferometric fringe fields obtained as the centre of the disc was displaced towards the viewer or image bundle $2.16\,\mu m$, $3.49\,\mu m$ and $8.89\,\mu m$ from its initial or reference position, while figure 3(*d*) shows a comparable double exposed holo-interferogram obtained with a centre displacement of $2.22\,\mu m$. Finally, in order to demonstrate the interferometer with somewhat more complex deformation fields, a stamped sheet metal disc (0.25 mm thickness) of 79 mm diameter was painted white and mounted in the inner ring of the gimballed holder. Figure 4(*a*) shows the resulting real-time interference fringe field due to a $4\,\mu m$ central displacement (out-of-plane) and a tilt of 0.00062° about its horizontal axis, while figure 4(*b*) shows the resulting fringe due to a $3.5\,\mu m$ out-of-plane displacement of a point 3 mm from the centre of the disc and a much greater tilt of 0.0012°. All of these real-time interferograms were recorded over an extended period of time (10 minutes to half an hour) with exposures of several seconds each.

5. Results and discussion

Figures 2, 3 and 4 show that reasonably high contrast, stable real-time fringe fields can generally be obtained using the simple but sophisticated RTF-HI system described in this report. Some apparent reduction in fringe contrast appears as either the tilt angle (figures 2(*a*), (*b*) and (*c*)) or the central displacement is

† Here the relatively flat surface of the test subject is aligned normal to the bisector of the illumination and observation directions, which intersect at ~9°.
‡ Spray painted white.
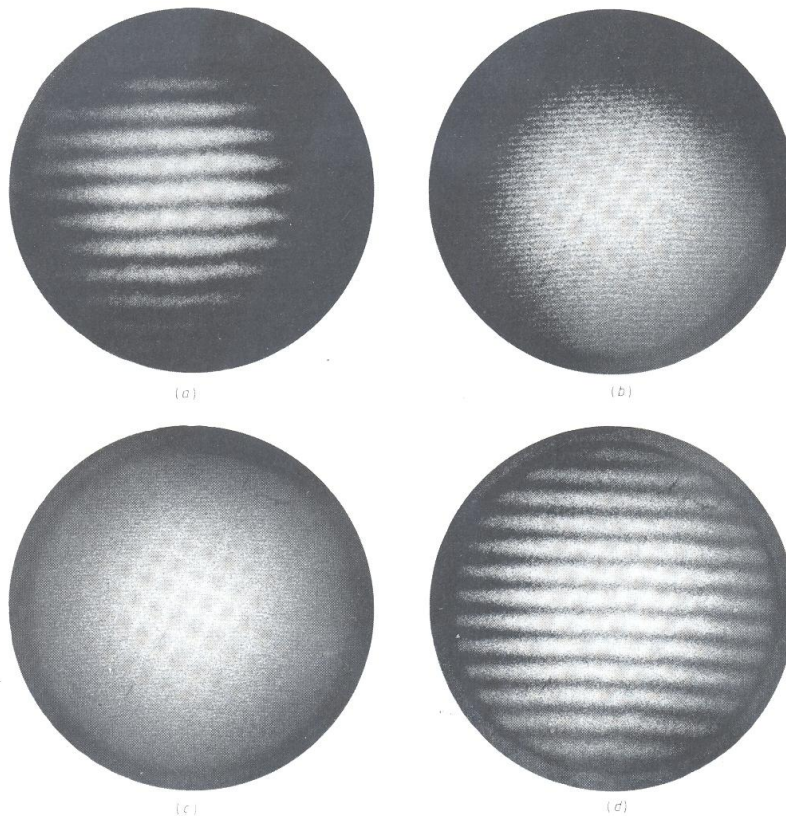§ Positioned to load the disc from behind through a 1 mm steel ball.

Figure 2. Holo-interferograms recorded through the RTF-HI system showing a glass disc tilted about a horizontal axis; (*a*) 0.044 mrad in real time, (*b*) 0.195 mrad in real time, (*c*) 0.278 mrad in real time, and (*d*) 0.047 mrad in double exposure.

increased (figures 3(*a*), (*b*) and (*c*)), but in every case readily resolvable fringes are present over the entire subject. Much of this apparent decrease in fringe contrast may be associated with limited resolution of the imaging bundle used in the RTF-HI system. Because this component breaks down the object image into discrete but imperfectly arrayed picture elements, there is always some blurring of the field and loss of definition. Naturally, this loss of definition becomes more apparent as the fringe frequency increases, and the fringe frequency increases as the tilt, or central loading, increases. Indeed, where the fringe frequency reaches the resolution limit of the image bundle the fringes fade out entirely and all that remains is the object image itself. This is so because, even though the interference fringes appear at the output end of the image bundle, and are not, themselves, transmitted through it, they still depend uniquely upon distributions of phase information which are themselves transmitted through the bundle in discrete elements. Consequently, the resolution of the interference fringes is limited by the resolution of the wavefronts from which they are derived. Moreover, there is some additional loss of fringe definition associated with changing fringe localisation (to be discussed below) which also contributes to an apparent loss of contrast, especially for the central loading tests (figure 3). However, comparing figures 2(*a*) and (*d*) or 3(*a*) and (*d*) it is also apparent that there is relatively little loss of contrast associated with operating in the more powerful real-time mode rather than the double exposure mode. Apparently, in the present system most of the induced phase drift differences associated with thermal effects on the fibre optic elements (Jones *et al* 1984) were so small as to have little or no significant influence on either the holograms themselves or the real-time holo-interferograms.

It was observed that the fringes formed during the rigid body tilt experiments localised very near the end of the bundle even at the larger tilt angles, whereas the out-of-plane displacement fields associated with the centre load tests generated fringe distributions which appeared to move away from the output end of the image bundle as the loading was increased. This behaviour mimics the fringe location phenomena observed in conventional holographic interferometry, and requires the same accommodation. It has long been known (Stetson 1969, 1970, Molin and Stetson 1970a, b, 1971) that in conventional holographic interferometers (that is, systems without a fibre optic image bundle between the object and the hologram), the fringes do not necessarily localise on the surface of the test subject. A pure rigid body translation, for example, will generate a fringe pattern at infinity, while a simple out-of-plane surface rotation will generate fringes that lie very near the object surface (either in front of, on, or behind it, depending on the observation direction), with fringes always localising on the surface along the axis of rotation. More complex surface movements and deformations may give rise to fringes which localise anywhere between plus and minus infinity (Vest 1979, Abramson 1981).

Such off-the-surface fringes often require an increased depth-of-field viewing/recording system to keep both them and the test surface in focus at the same time so as to ensure high contrast and the resolution of detail. Such depth-of-field requirements necessitate a reduction in system aperture, which unfortunately leads to a significant coarsening of the coherent speckle pattern (Collier *et al* 1971, Dainty 1975) and once again an associated loss of resolution and contrast. Consequently, in both
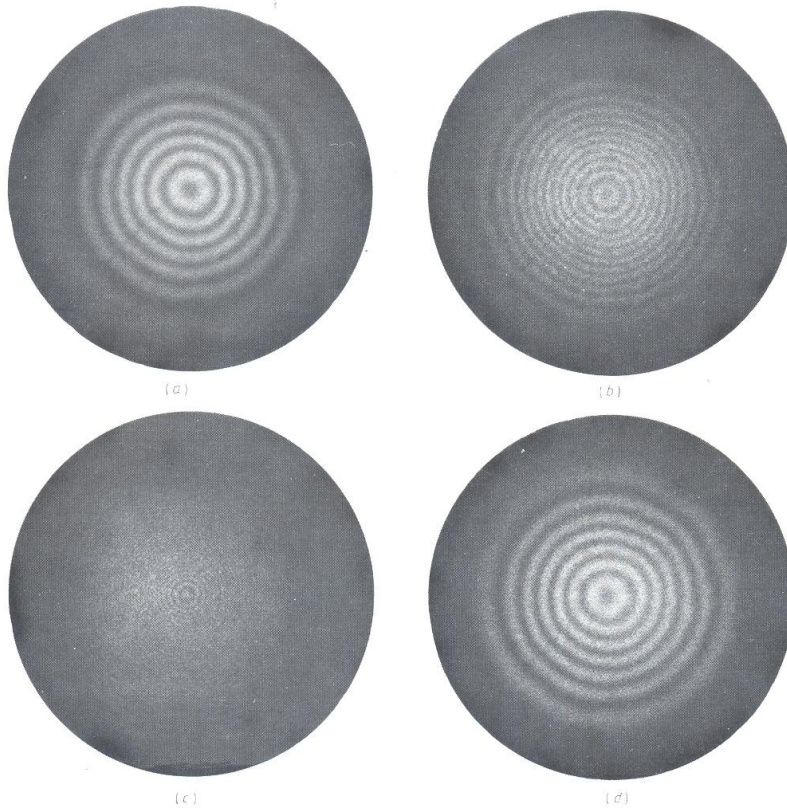

Figure 3. Holo-interferograms recorded through the RTF-HI system showing a centrally loaded glass disc at peak out-of-plane displacements of: (*a*) 2.16 μm in real time, (*b*) 3.49 μm in real time, (*c*) 8.87 μm in real time, and (*d*) 2.27 μm in double exposure.
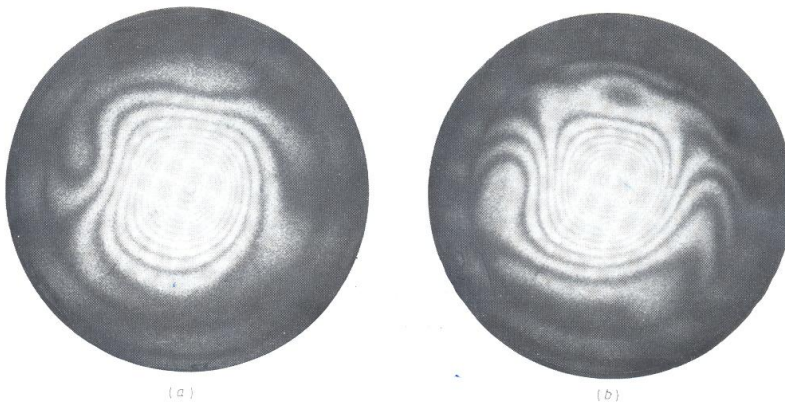

Figure 4. Real-time holo-interferograms recorded through the RTF-HI system showing a metal disc loaded: (*a*) centrally to 4 μm out-of-plane displacement and simultaneously tilted 0.011 mrad about a horizontal axis, and (*b*) 3 mm off centre to a 3.5 μm out-of-plane displacement and simultaneously tilted 0.022 mrad about a horizontal axis.

conventional HI and RTF-HI systems, the observation and reading of high frequency off-the-surface fringes frequently requires some sacrifice in focus, with an unavoidable loss of contrast, in order to suppress the speckle effects and achieve resolvable results. In the present RTF-HI experiments this necessitated some reduction in aperture (to increase the depth-of-field) and refocusing off the output end of the image bundle during these tests in order to record figures 3(*a*), (*b*) and (*c*). Nevertheless, both experiments achieved a maximum fringe density slightly greater than one per millimetre† as seen in figures 2(*c*) and 3(*c*). On the image bundle (output end surface) itself this represents almost ten real-time interference fringes per millimetre, about one-third of the theoretical maximum of 30 lines per millimetre (based on the image bundles' nominal resolution). Finally, in the experiments with the disc shown in figure 4, it was found that the appropriate combination of out-of-plane loading and tilt could be made to generate relatively complex high contrast, stable real-time interference fringe patterns that were well localised near the output end of the image bundle (yet far removed from the actual test subject).

References
Abramson N 1981 *The Making and Evaluation of Holograms* (New York: Academic) pp 70–267

Caufield H J 1979 *Handbook of Optical Holography* (New York: Academic) pp 463–502

Collier R J, Burckhardt C B and Lin L H 1971 *Optical Holography* (New York: Academic) pp 418–44, 347–8

Dainty J C 1975 *Laser Speckle and Related Phenomena* (New York: Springer-Verlag) p 207

Dudderar T D and Gilbert J A 1983 Fiber optic pulsed laser holography
Appl. Phys. Lett. **43** 730–2

Dudderar T D, Gilbert J A and Boehnlein A J 1983 Achieving stability in remote holography using flexible multimode image bundles
Appl. Opt. **22** 1000–5

Dudderar T D, Gilbert J A, Franzel R A and Schamell J H 1984 Remote vibration measurement by time averaged holographic interferometry
Proc. 5th Int. Congress on Experimental Mechanics, Montreal, Ontario, Canada

Erf R K 1974 *Holographic Nondestructive Testing* (New York: Academic) pp 87–103

Gilbert J A, Dudderar T D and Boehnlein A J 1984 Ultra low-frequency holographic interferometry using fibre optics
Optics and Lasers in Eng. **5** 29–40

Gilbert J A, Dudderar T D and Nose A 1983a Remote displacement analysis through different media using fiber optics
Proc. 1983 Spring Conf. on Exp. Mech., SESA, Cleveland, OH 424-430 submitted to *Opt. Eng.*

Gilbert J A, Dudderar T D, Schultz M E and Boehnlein A J 1983b The monomode fiber – a new tool for holographic interferometry
Exp. Mech. **23** 190–5

Gilbert J A and Herrick J W 1981 Holographic displacement analysis with multimode-fiber optics
Exp. Mech. **21** 315–20

Gilbert J A, Schultz M E and Boehnlein A J 1982 Remote displacement analysis using multimode fiber-optic bundles
Exp. Mech. **22** 398–400

Hadawnik D 1976 Holographische Endoskopie
Optik **45** 21–38

Hall P M, Dudderar T D and Argyle J F 1983 Thermal deformation observed in leadless ceramic chip carriers surface mounted to printed wiring boards
IEEE Trans. Components, Hybrids, and Manufacturing Technology **CHMT-6** 544–52

Jones J D C, Corke M, Kersey A D and Jackson D A 1984 Single-mode fibre-optic holography
J. Phys. E: Sci. Instrum. **17** 271–3

Leite A M P P 1979 Optical fiber illuminators for holography
Opt. Commun. **28** 303–6

Molin N-E and Stetson K A 1970a Measurement of fringe loci and localization in hologram interferometry for pivot motion, in-plane rotation, and in-plane translation, Part I
Optik **31** 157–77

Molin N-E and Stetson K A 1970b Measurement of fringe loci and localization in hologram interferometry for pivot motion, in-plane rotation, and in-plane translation, Part II
Optik **31** 281–91

Molin N-E and Stetson K A 1971 Fringe localization in hologram interferometry of mutally independent and dependent rotations around orthogonal, non-intersecting axes
Optik **33** 399–422

Powell R L and Stetson K A 1965 Interferometric analysis by wavefront reconstruction
J Opt. Soc. Am. **55** 1593–8

Rosen A N 1975 Holographic fundoscopy with fiber optic illumination
Opt. Laser Technol. **7** 3

Rowley D 1983 The use of a fiber-optic reference beam in a focused image holographic interferometer
Opt. Laser Technol. **15** 194–8

Stetson K A 1969 A rigorous theory of the fringes in hologram interferometry
Optik **29** 386–400

Stetson K A 1970 The argument of the fringe function in hologram interferometry of general deformations
Optik **31** 576–91

Stetson K A and Powell R L 1965 Interferometric hologram evaluation and real-time vibration analysis of diffuse objects
J. Opt. Soc. Am. **55** 1694–5

Suhara T, Nishihara H and Koyama J 1977 Far radiation field emitted from an optical fiber and its applications to holography
Trans. IECE Japan, Sec E (Engl) **60** 533–40

Vest C M 1979 *Holographic Interferometry* (New York: Wiley) pp 107–45

Yonemura M, Nishisaka T and Machida H 1981 Endoscopic hologram interferometry using fiber optics
Appl. Opt **28** 1664–7

† As measured on the original interferograms recorded at 0.9 magnification.